Global Journal of Researches in Engineering
Mechanical and Mechanics Engineering
Volume 12 Issue 7 Version 1.0 Year 2012
Type: Double Blind Peer Reviewed International Research Journal
Publisher: Global Journals Inc. (USA)
Online ISSN: 2249-4596 Print ISSN:0975-5861

CFD Analysis of Solid Fuel Scramjet Combustors

By Probhas Bose, K.M.Pandey & K.O.Reddy

Research scholar Dept of Mech Engg, N.I.T Silchar, Assam, India

Abstract - The combustion of a solid fuel under supersonic cross flow conditions was investigated theoretically. A two-dimensional, axisymmetric, turbulent (k - **ε**), global one step reaction model was solved numerically. Numerical simulations of the combustor geometries presenting the situations with solid fuel regression were conducted using FLUENT software. The combustor inlet airflow had a Mach number of 2, total temperature of 1200 K and total pressure of 30 atm. The HTPB fuel and a global one step reaction mechanism were used. The results of non reacting computation reveal that the airflow velocity deceases in the majority zone of combustor with the solid fuel boundary regression. The results of reacting computation reveal that the supersonic zone in the divergent section of the case gets larger than non reaction case. Combustion takes place in the vicinity of solid fuel wall.

Keywords : *scramjet; solid fuel; combustor; CFD analysis, mach number.*

GJRE-A Classification : *FOR Code: 299902p*

Strictly as per the compliance and regulations of :

CFD Analysis of Solid Fuel Scramjet Combustors

Probhas Bose [α], K.M.Pandey [σ] & K.O.Reddy [ρ]

Abstract - The combustion of a solid fuel under supersonic cross flow conditions was investigated theoretically. A two-dimensional, axisymmetric, turbulent (k - ε), global one step reaction model was solved numerically. Numerical simulations of the combustor geometries presenting the situations with solid fuel regression were conducted using FLUENT software. The combustor inlet airflow had a Mach number of 2, total temperature of 1200 K and total pressure of 30 atm. The HTPB fuel and a global one step reaction mechanism were used. The results of non reacting computation reveal that the airflow velocity deceases in the majority zone of combustor with the solid fuel boundary regression. The results of reacting computation reveal that the supersonic zone in the divergent section of the case gets larger than non reaction case. Combustion takes place in the vicinity of solid fuel wall.

Keywords : scramjet; solid fuel; combustor; CFD analysis, mach number.

I. Introduction

As flight Mach number is increased beyond the area of Mach 5, the hypersonic phenomena that begin to occur reduce significantly the performance of conventional ramjet engines with a subsonic flow combustion chamber. The demand for cost reduction and increased dependability of transporting payload to orbit has led to a constantly increasing interest in development of modern air breathing propulsion systems for hypersonic vehicles. Consequently, attention is being focused on the supersonic combustion ramjet (commonly known as scramjet). Ramjet engines operate at supersonic flight Mach numbers. In the conventional ramjet, the air flow is slowed down to subsonic flow velocities throughout the combustion chamber in order to achieve better flame stabilization and combustion efficiencies. However, for flight Mach numbers above 5, better performance (higher specific impulse) can be achieved if the combustor flow Mach number remains supersonic [1,2].The scramjet engine is usually powered by liquid fuels. For certain applications, however, one can see an advantage in employing solid fuels. The system design is greatly simplified, storage is very convenient, and a feeding system is not required. Hence, low cost propulsion system is enabled. However, unlike the case of liquid fuel combustion, the use of a solid fuel gives no direct control on fuel flow rate and injection velocity. The solid fuel undergoes degradation and gasification because of heat feedback from the hot gas flow, resulting in regression of the solid wall and establishment of diffusion flame within the boundary layer above the wall. Flame holding is achieved by the inlet step.

II. Literature Review

Scramjet (supersonic combustion ramjet) has proposed and is regarded as one of best propulsion systems for hypersonic flight. [1] Up to date scramjets with liquid fuel (e.g. kerosene) and gaseous fuel (e.g. hydrogen) have been studied widely. [2] In 2004 the liquid-hydrogen-fueled NASA X-43A scramjet flight vehicle performed two record breaking speed (Mach 7 and 10) self propelled flights, demonstrating the scramjet concept in actual flight conditions.[3, 4] At present there are still many research projects for hypersonic fight vehicle in America, including Hyfly, X-51A, FALCON and so on. [5] Reports related to solid fuel scramjet research, theoretical or experimental, are quite scarce in the open literature.

The use of solid fuels is widespread in conventional ramjet engines providing it with desirable characteristics: high energy density resulting in a more compact system, simplicity (no need of fuel tanks and feeding systems), safety, easy storage for long duration and finally, readiness upon demand. Consequently, the solid fueled scramjet engine should extend the operating limits of solid fuel oriented vehicles, such as missiles, boosters and sustainers and projectiles, into the hypersonic flight regime. [6] The direct-connect combustor tests and numerical simulations of combustor have been developed. In the direct-connect combustor tests, combustors have similar axisymmetric geometry sketched as Fig.1. The fuel grain contains three main sections. At the forward end air from the diffuser (or the air heater in the test system) enters at supersonic velocity and encounters a recess having a backward facing step at its head end and an oblique step at its rear. This arrangement causes some of the air to circulate near the walls, while in the center the flow remains supersonic. This section is essential for flame holding and it was found to enable self ignition of the fuel when the total temperature of the incoming air

Author α : Research scholar Dept of Mech Engg, N.I.T Silchar, Assam, India.
Author σ : Professor, N.I.T Silchar, India.
E-mail : kmpandey2011@yahoo.com
Author ρ : PG Student Dept of Mech Engg, N.I.T Silchar.
E-mail : obulareddy.bec10@gmail.com

exceeds 1000K. The next part is a cylindrical section having a diameter smaller than the entrance chamber, in order to prevent the flow from accelerating too much. The final section of the fuel grain is a divergent cone, to prevent thermal chocking due to heat addition at supersonic velocities.[7]

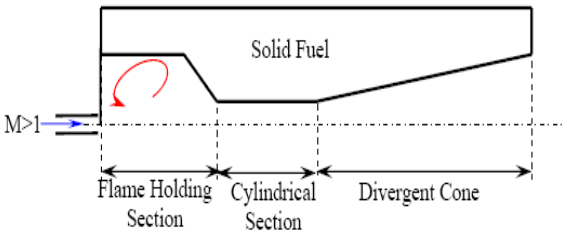

Fig. 1 : Solid fuel scramjet combustor geometry

Two type of solid fuels have been used in direct-connect combustor tests: Plexiglas (PMMA) and hydroxyl-terminated polybutadiene (HTPB). The advantage of using Plexiglas, despite its low energetic properties, is that due to its high mechanical strength there is no need for outer casing and its transparency enables observation of the flow and combustion phenomena within its axisymmetric bore.[6] Figure 1. Schematic geometry of the solid fuel scramjet combustor Gany et al from Israel Institute of Technology have conduced plentiful direct-connect combustor tests. Self-ignition and sustained combustion of PMMA with no external aid (such as reactive gas injection or a pilot flame) were demonstrated, flame holding limits were determined experimentally and temporal and spatial fuel regression rate data were obtained by video recording. [8] Direct-connect tests of Metallized and non metalized HTPB scramjet combustor have also been conducted. Aluminum powder was used as the metal fuel additive. Self ignition and stable combustion of both metalized and non metalized fuels has been achieved. Results show that the regression rate of metalized fuel is slightly higher. The addition of aluminum particles improved the specific thrust (thrust per air mass flow rate), while decreasing the specific impulse.[7] The objective of the present research is to determine the feasibility of numerical simulation by CFD software FLUENT and analyze the flow field of scramjet combustor, based on the combustor model and experimental data of Ref. 7.

Truck mounted multi barrel rocket launcher (MBRL) is an area weapons which is capable of launching free flight rockets (FFR) at the target from a distance of 30 – 40 km. In addition to conventional warheads, it also has the capability to deliver nuclear war head [8]. Brassey's Encyclopedia of Land Forces & Warfare [9] brought out that despite logistical penalties and the ease of detection, MBRLs are favoured by Western armies in place of heavy guns. FFR motors use solid propellants as it possess well defined, reproducible, and near constant rate of burning, non hygroscopicity, ability to be worked into grain of widely varying sizes, shapes and burning times. It has adequate mechanical and physical properties and have sufficient strength to prevent sagging at higher temperatures, or imbrittlement at low temperatures [10]. The major problems here as observed by MacLaren AJ et-al [11] is mid course thrust control as burning rate of propellant cannot be altered unlike its liquid counterpart; the other problem being low specific impulse. However, Fleeman EL [12] suggested three approaches for mid air control. These are use of pulsed and pintle motors and gel propellant. Guery JF et-al [13] brought out generation of high specific impulse and restart capabilities by liquid propellant. The specific impulses of solid propulsion systems are 20% and 80% lower than that of liquid and cryopropulsion systems, respectively. However, in this case the system is more complex and expensive states Gupta et-al [14]. Lipanov AM observed that once ignited, solid propellant usually burns smoothly at a predetermined rate on all the exposed surfaces of the grain [15]. For rocket launcher application the requirement is of constant thrust which is met by neutral burning surface.

Rossi et-al [16] established that in the class of solid fuels composite propellant is preferred. It presents the main advantage of low vulnerability and high specific impulse. Moreover, properties of composite propellant may be tailor made by changing the compositions and compound rate. It is composed of one binder (typically, Polybutadiene or glycidyle azide polymer), one oxidizer (typically NH_4ClO_4) and one fuel (Al, Zr or Mg). The metallic particles remain after combustion may cause damage to the nozzle if flight duration is considerable. However, in case of MBRL, small duration of burning and expelling of burning gases quickly does not provide adequate time to cause damage to the nozzle.

Nair UR [17] observed composite propellants have acquired greater significance because of advantage of wide range of mechanical properties and superior strain capability compared to conventional propellants in addition to higher delivered I_{sp}. For realizing smokeless exhaust Tarver CM et-al [18]explored RDX and HMX. It is observed that addition of combination of AP and nitramines improves the I_{sp} marginally. Tian Y et-al [19] and Florczak B [20] found superior performance level by replacing hydroxy-terminated polybutadine (HTPB) binder by energetic polymer systems comprising of GAP and BAMO copolymers as polymer matrix in combination with TMETN/TEGDN/ BTTN/BDNPF/A as plasticizers.

Although materials like CL-20, FOX-7 was synthesized as an explosive of interest. It has also been evaluated as a component of propellants. Floreszek B [21] and Mueller D [22] have reported the effect of replacement of AP by FOX-7 in slurry cast composition. They determined burning rate of the propellant in sub scale rocket motor and observed marginal decrease in it

on replacement of AP by FOX-7. It is predicted that a combination of HNF / ADN with energetic binders like GAP, BAMO, NIMMO can offer I_{SD} of the order of 300 s. However, Chen JK [23] and Hsieh WH [24] suggested validation such claim in a practically useful propellant.

Chatillon C [25] observed that unlike the other ingredients, aluminum particles can burn in a signficant portion of the chamber and produce a condensed phase that is carried out into the flowfield. Thereby, aluminum particles can affect appreciably combustion instabilities by acting as driving or, on the contrary, as damping mechanisms.

Use of eco friendly propellant is advocated by Mahanta A [26] as with AP oxidizer it emits plumes containing HCl. Addition of magnesium neutralized plumes in the range of 1-10 %, while sodium nitrate scavenged propellants (HTPB/$NaNO_3$/AP/Al) have the potential of reducing it by about 1 - 3 %.

Design of a solid propellant grain is governed by ballistic, processing, and structural integrity requirements. Pressure-time, thrust-time, acceleration, velocity, and trajectory are decided by propellant configuration, and are largely a geometric consideration. Shekhar H [27] proposed funnel port tubular propellant grain for neutral burning. Pressure developed by the burning of propellant depends upon along with other parameters geometry of the grain. Relation between web and mass burnt is established by form function relation; relation between web and surface area is established [28] by surface area relation. EgonG et-al [29] suggested a test method for service life prediction of propellant. Shekhar H [30] observed that an HTBP composite propellant behaves as compressible material in most of the regionsand near-failure region or at higher strains; Poisson's ratio is near 0.25. Miloš Predrag [31] suggested a specific methodology for optimization of star shape propellant grains in the sense of minimizing stress and strain without compromising the required internal ballistic performances. The design of solid propellant grain that provides neutral burning is important to optimize rocket motor performance.

III. Scramjet Combustor Geometry

The computational domain of the geometry and the governing equations of the solver are explained in this session, the schematic diagram of the scramjet combustor computational domain is shown below

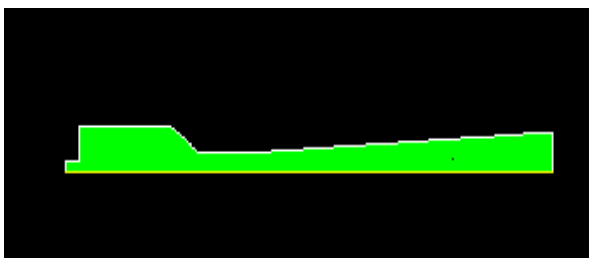

Fig. 2 : Computational domain grid generation

IV. Classification Of Solid-Propellant Combustion Models

Existing models of solid-propellant combustion can be broadly classified into three general categories: (1) simple models that do not account for chemical kinetics and typically solve only the mass and energy equations in the condensed and gas phases; (2) global-kinetics models based on simplified chemical reaction mechanisms in either, or in both, the gas and condensed phases; and (3) detailed models with elementary kinetics mechanisms in the gas phase, and thermal decomposition and subsequent reactions in the condensed phase. In addition, various ignition models have also been developed. Most of the existing analyses use global reactions to simulate ignition, but some recent efforts have modeled the entire process of ignition with detailed kinetics.

a) Combustion models based on global kinetics

Models of this type treat reduced chemical kinetics and solve both the energy and species transport equations. Global kinetics is immensely useful for multi-dimensional modeling, where the use of detailed mechanisms is not viable due to numerical stiffness problems attributed to the wide variety of time and length scales involved and limited computing sources.

V. Numerical Method

CFD software FLUENT was employed to compute the non reacting and reacting flow field of the above combustor. The inlet airflow has a Mach number of 2, total temperature of 1200 K and total pressure of 30 atm, which is identical to inflow conditions in Ref.7. In the simulation, solid fuel grain boundary was set to mass flow inlet with mass flow rate of 0.0197 kg/s. The pressure of combustor outlet was set to 1 atm. The two-equation RNG k-ε model was used to model the turbulence and standard wall functions were used to model the flow near the wall. Because of axisymmetry of model, only half of the combustor symmetry was computed. The entire computational domain was discretized using a total mesh size of 5,210. In the simulation of reacting flow field, HTPB was supposed that its pyrolysis only produced one gas C4H6. The combustion of C4H6 was modeled using a global one-step reaction mechanism, assuming complete conversion of the fuel to CO2 and H2O. The reaction equation is

$$C4H6+5.5O2 \rightarrow 4CO2+3H2O$$

This reaction was defined in terms of stoichiometric coefficients, formation enthalpies, and parameters that control the reaction rate. The reaction rate was determined assuming that turbulent mixing is the rate-limiting process, with the turbulence-chemistry interaction modeled using the eddy dissipation model.

a) The two-equation RNG k-ε model

The RNG model was developed using Re-Normalisation Group (RNG) methods by Yakhot et al to renormalise the Navier-Stokes equations, to account for the effects of smaller scales of motion. In the standard k-epsilon model the eddy viscosity is determined from a single turbulence length scale, so the calculated turbulent diffusion is that which occurs only at the specified scale, whereas in reality all scales of motion will contribute to the turbulent diffusion. The RNG approach, which is a mathematical technique that can be used to derive a turbulence model similar to the k epsilon, results in a modified form of the epsilon equation which attempts to account for the different scales of motion through changes to the production term.

By definition, two equation models include two extra transport equations to represent the turbulent properties of the flow. This allows a two equation model to account for history effects like convection and diffusion of turbulent energy.

Most often one of the transported variables is the turbulent kinetic energy, k. The second transported variable varies depending on what type of two-equation model it is. Common choices are the turbulent dissipation, ϵ, or the specific dissipation, ω. The second variable can be thought of as the variable that determines the scale of the turbulence (length-scale or time-scale), whereas the first variable, k, determines the energy in the turbulence.

i. *Transport Equations*

There are a number of ways to write the transport equations for k and ϵ, a simple interpretation where bouyancy is neglected is

$$\frac{\partial}{\partial t}(\rho k)+\frac{\partial}{\partial x_i}(\rho k u_i)=\frac{\partial}{\partial x_j}\left[\left(\mu+\frac{\mu_t}{\sigma_k}\right)\frac{\partial k}{\partial x_j}\right]+P_k-\rho\epsilon$$

$$\frac{\partial}{\partial t}(\rho\epsilon)+\frac{\partial}{\partial x_i}(\rho\epsilon u_i)=\frac{\partial}{\partial x_j}\left[\left(\mu+\frac{\mu_t}{\sigma_\epsilon}\right)\frac{\partial\epsilon}{\partial x_j}\right]+C_{1\epsilon}\frac{\epsilon}{k}P_k-C_{2\epsilon}^{*}\rho\frac{\epsilon^2}{k}$$

where $C_{2\epsilon}^{*}=C_{2\epsilon}+\dfrac{C_\mu\eta^3(1-\eta/\eta_0)}{1+\beta\eta^3}$

and $\eta=Sk/\epsilon$ and $S=(2S_{ij}S_{ij})^{1/2}$

With the turbulent viscosity being calculated in the same manner as with the standard k-epsilon model.

Constants

It is interesting to note that the values of all of the constants (except β) are derived explicitly in the RNG procedure. They are given below with the commonly used values in the standard k-epsilon equation in brackets for comparison:

$C_\mu=0.0845$ (0.09)
$\sigma_k=0.7194$ (1.0)
$\sigma_\epsilon=0.7194$ (1.30)
$C_{\epsilon1}=1.42$ (1.44)
$C_{\epsilon2}=1.68$ (1.92)
$\eta_0=4.38$
$\beta=0.012$ (derived from experiment)

b) Governing equations for compressible flow

For all flows, FLUENT solves conservation equations for mass and momentum. For flows involving heat transfer or compressibility, an additional equation for energy conservation is solved. For flows involving species mixing or reactions, a species conservation equation is solved.

i. *Non reacting flow*

In fluid dynamics, the continuity equation states that, in any steady state process, the rate at which mass enters a system is equal to the rate at which mass leaves the system.
The differential form of the continuity equation is

$$\frac{\partial\rho}{\partial t}+\nabla\cdot(\rho\mathbf{u})=0$$

where

- ρ is fluid density,
- t is time,
- $\mathbf{u}$ is the flow velocity vector field.

Momentum equation

$$\frac{\partial(\rho u)}{\partial t}+\nabla\cdot(\rho uv)=-\frac{\partial P}{\partial x}+\frac{\partial\tau_{xx}}{\partial x}+\frac{\partial\tau_{yx}}{\partial y}+\rho f_{xx}$$

Energy equation

$$\rho\frac{Dq}{Dt}=\rho\frac{D}{Dt}\left\{i+V+\frac{1}{2}u_iu_i\right\}+\frac{\partial}{\partial x_i}(pu_i)-\frac{\partial}{\partial x_j}(\tau_{ij}u_i)$$

or

$$\rho\frac{D}{Dt}\left[\frac{u_iu_i}{2}+e\right]-\rho k_iu_i-\frac{\partial}{\partial x_j}[\tau_{ji}u_i]+\frac{\partial q_i}{\partial x_i}=0,$$

ii. *Reacting flow*

Among all the above three equations there are two more equations for species transport model. When you choose to solve conservation equations for chemical species, FLUENT predicts the local mass fraction of each species, Yi, through the solution of a convection-diffusion equation for the ith species. This conservation equation takes the following general form:

$$\frac{\partial}{\partial t}(\rho Y_i)+\nabla\cdot(\rho\vec{v}Y_i)=-\nabla\cdot\vec{J}_i+R_i+S_i$$

Where Ri is the net rate of production of species i by chemical reaction (described later in this section) and Si is the rate of creation by addition from the dispersed phase plus any user-defined sources. An equation of this form will be solved for N-1 species where N is the total number of fluid phase chemical species present in the system. Since the mass fraction of the species must sum to unity, the Nth mass fraction is determined as one minus the sum of the N - 1 solved mass fractions. To minimize numerical error, the Nth species should be selected as that species with the overall largest mass fraction, such as N2 when the oxidizer is air.

Mass Diffusion in Turbulent Flows

In turbulent flows, FLUENT computes the mass diffusion in the following form:

$$\vec{J}_i = -\left(\rho D_{i,m} + \frac{\mu_t}{\mathrm{Sc}_t}\right)\nabla Y_i$$

Where Sct is the turbulent Schmidt number ($\frac{\mu_t}{\mathrm{Sct}}$ where μ_t is the turbulent viscosity and Dt is the turbulent diffusivity). The default Sct is 0.7. Note that turbulent diffusion generally overwhelms laminar diffusion, and the specification of detailed laminar diffusion properties in turbulent flows is generally not warranted.

VI. Simulation Results

a) Non Reacting Flow field

Non reacting flow field of the model were computed by setting solid fuel boundary to wall. Fig.3 shows cold flow field of the combustor geometry without fuel addition or reaction. From Fig. 3 Mach number map, it can be seen that inflow air was expanded at step corner and airflow Mach number increased from 2.0 to 2.5. Velocity is very low and static temperature is very high to 1150 K (Fig.4) in the recirculation zone. The high temperature is enough to ignite the solid grain. In the cylindrical section airflow has a maximum Mach number of 1.9. In the divergent section airflow is expanded largely with Mach number of combustor exit up to 3.4.

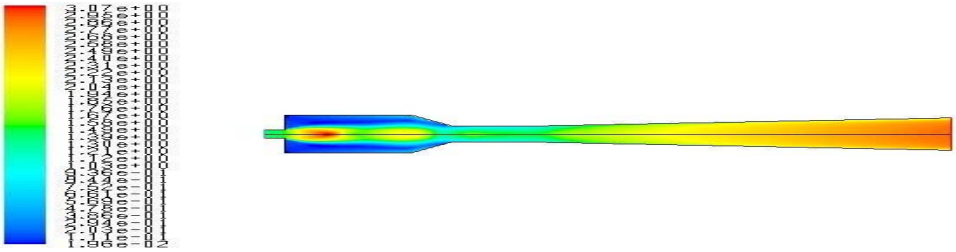

Fig. 3 : Mach number contour

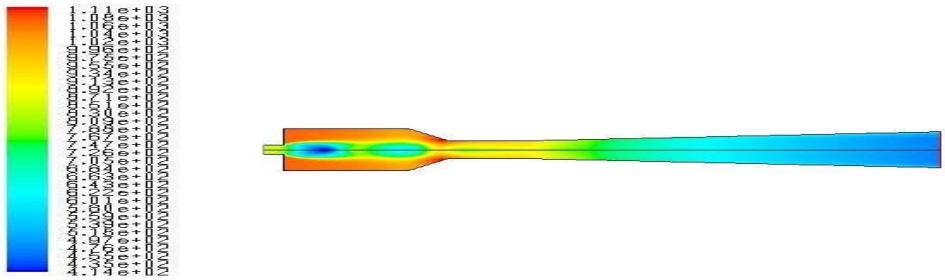

Fig. 4 : Static temperature contour

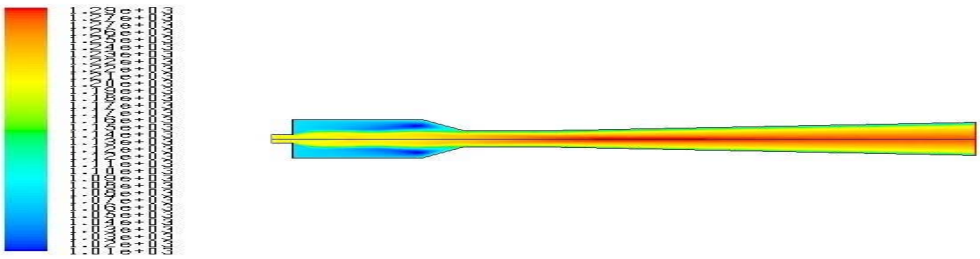

Fig. 5 : Total temperature contour

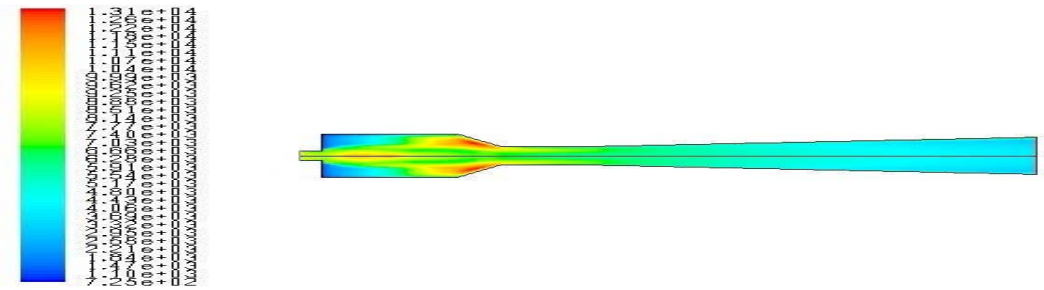

Fig. 6 : Turbulent intensity contour

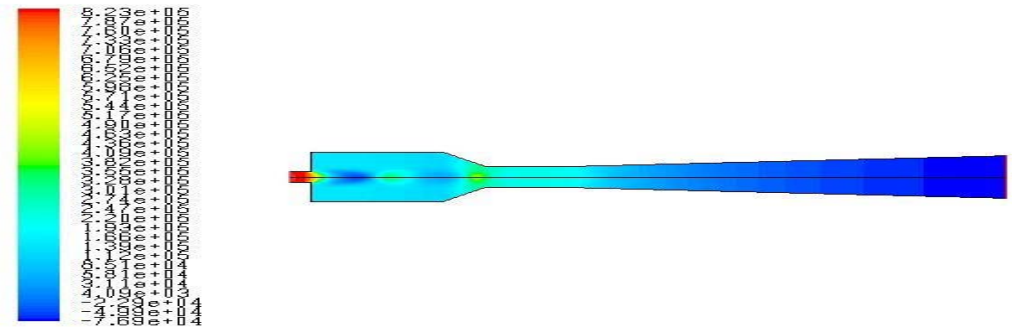

Fig. 7 : Static Pressure Contour

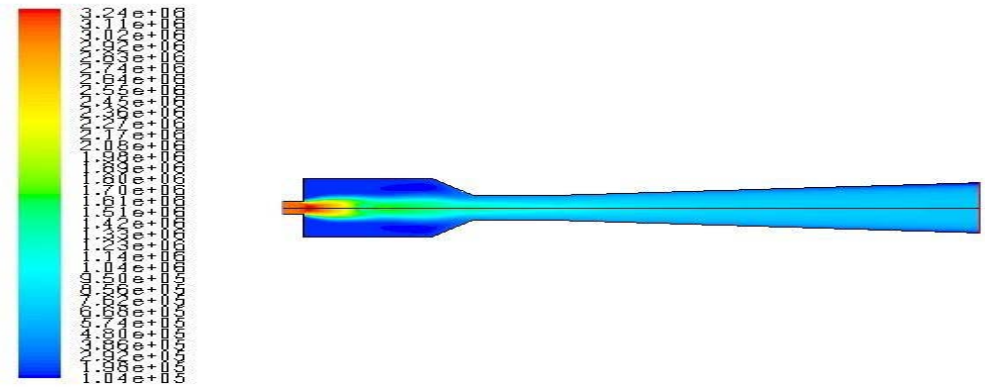

Fig. 8 : Total Pressure Contour

b) Reacting Flow field

Reacting flow fields of three combustor geometries are obtained by the reaction of C4H6 and O2. Fig.7-8 shows reacting flow field contours.

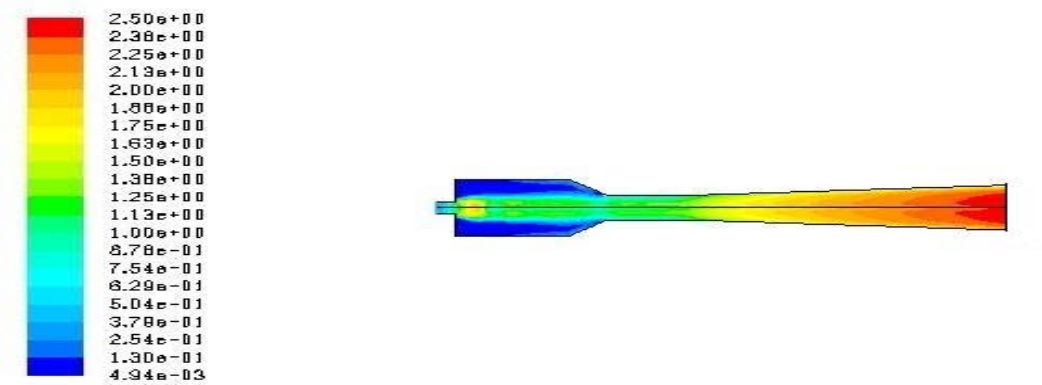

Fig. 9 : Mach Number Contour

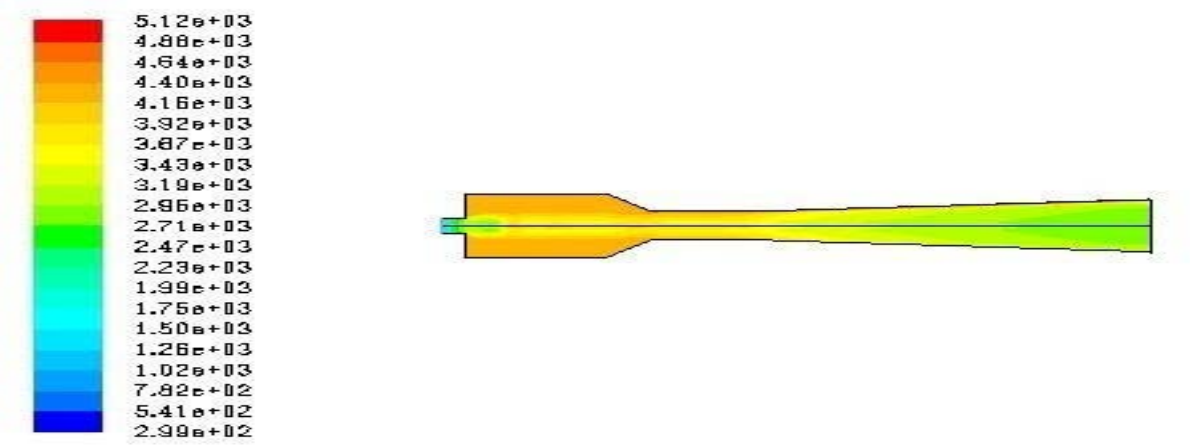

Fig. 10 : Static Temperature Contour

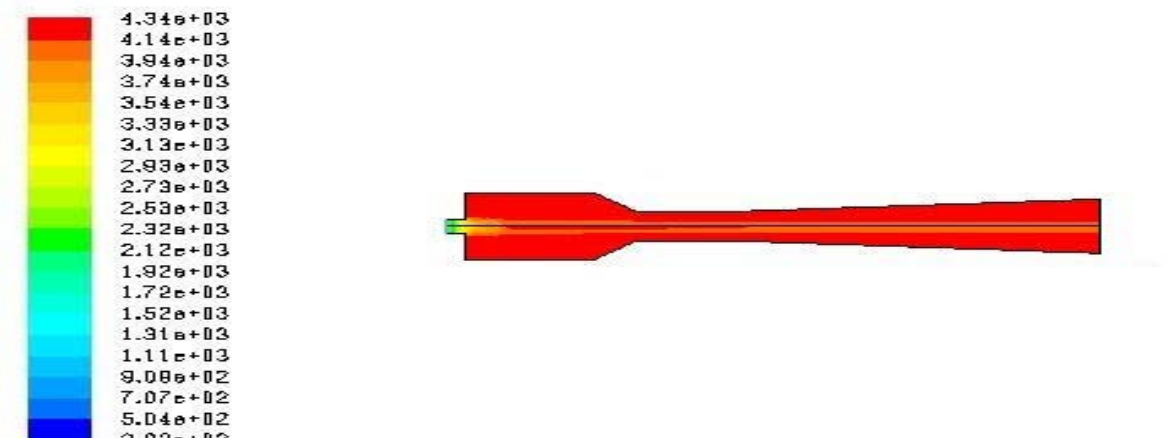

Fig. 11 : Total Temperature Contour

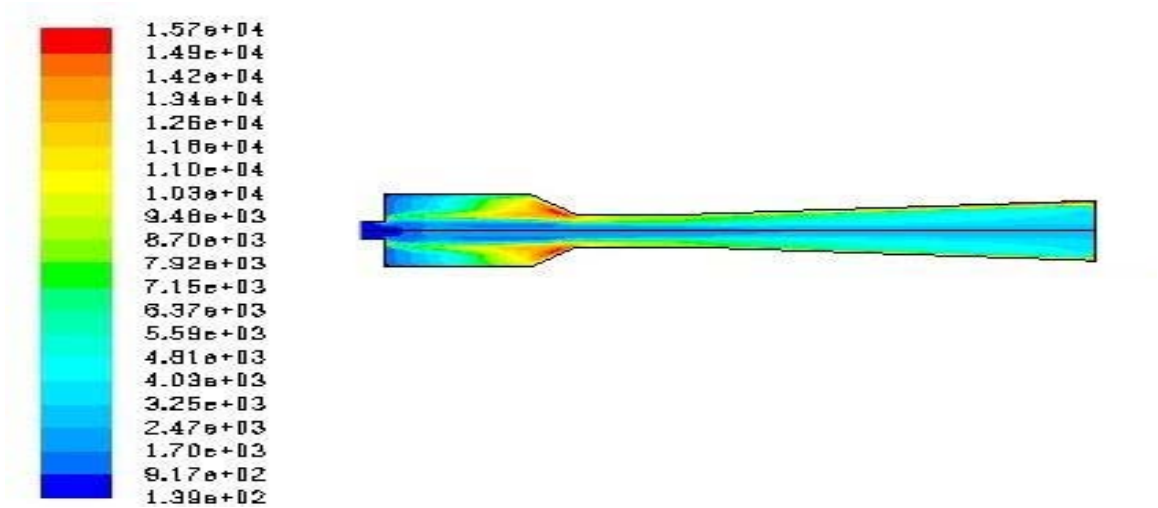

Fig. 12 : Turbulent Intensity Contour

VII. Results Discussion

a) Mach number

Figures 3 and 7 present the flow Mach number distribution of a non-reacting case and that of the present reacting case, respectively. Comparison reveals that the velocity field changes substantially. The inlet fan at the step corner, which served to elevate the Mach number from 2 to a maximum value of 3.07 in the non-reacting case, almost disappears in the reacting case, resulting in a maximum Mach number of 2.1. Broad

areas of supersonic flow in the non-reacting case become subsonic due to the heat release from the chemical reactions. A mixed supersonic (at the center)/subsonic (at the circumference) jet is formed at the combustor exit when combustion takes place, replacing the almost whole supersonic non-reacting stream.

b) Temperature

Temperature distribution of the reacting flow field is presented in Fig. 10 and 11. The computation results reveal that sustained combustion can exist within the combustor for the inlet and geometry conditions under investigation. A diffusion flame with a maximum temperature of 3500K is formed supplying a substantial heat addition to the flow. The static and stagnation temperatures increase from 300 K and 1300 K at the inlet to mass-averaged values of 3150 K and 3450 K, respectively. The region between the wall and fame center is heated too due to the chemical reactions and the lateral heat transfer from the flame. At the combustor axis, the temperature remains almost unchanged.

c) Turbulent Intensity

The turbulent intensity is increasing from the intake to the section head of the cylinder and the value is higher as compared to the in other locations that means at the wall boundaries the turbulent value is decreases due to standard wall functions and in the case of reaction flow field the turbulent intensity .

VIII. Conclusion

Comparison of reacting and non reacting flow Mach numbers reveal that the velocity field changes substantially. The inlet fan at the step corner, which served to elevate the Mach number from 2 to a maximum value of 3.07 in the non-reacting case, almost disappears in the reacting case, resulting in a maximum Mach number of 2.1. Broad areas of supersonic flow in the non-reacting case become subsonic due to the heat release from the chemical reactions. A mixed supersonic (at the center)/subsonic (at the circumference) jet is formed at the combustor exit when combustion takes place, replacing the almost whole supersonic non-reacting stream. The computation results reveal that sustained combustion can exist within the combustor for the inlet and geometry conditions under investigation. A diffusion flame with a maximum temperature of3500 K is formed supplying a substantial heat addition to the flow. The static and stagnation temperatures increase from 300 K and 1300 K at the inlet to mass-averaged values of 3150 K and 3450 K, respectively. The region between the wall and fame center is heated too due to the chemical reactions and the lateral heat transfer from the flame. At the combustor axis, the temperature remains almost unchanged.

The pressure in combustion chamber is explained as static and total pressure. For the case of non reacting flow field the static and total pressure contours are shown in Fig 7-8.

The pressure in non reacting flow is accrued an value of 40 atmospheric pressure. Where as in reacting flow the combustion chamber pressure is more high due to the chemical specie reaction and gaseous products.

The turbulent intensity behavior of non reacting flow can be explained from the turbulent intensity contours as shown above. From non reacting flow field can we say that the turbulent intensity accrued a maximum value in the flame holding section and at the cylinder head inlet. But in the case of reacting the turbulent intensity is more higher as compared to the non reacting case.

References Références Referencias

1. William, H.Heiser and David, T. Pratt. “Hypersonic Airbreathing Propulsion”. AIAA Education Series, 1994.
2. Curran, E. T. and Murthy, S. N. B. “Scramjet Propulsion”. Volume 189, AIAA Inc. Washington D C, USA, 2002.
3. Michael A Dornheim. “X-43 Flight Test Indicates Thrust is Greater Than Drag”. Aviation Week &Space Technology, April 5, 2004, pp. 28-29.
4. Michael A Dornheim. “NASA's X-43A Hyper-X Reaches Mach10 in Flight Test”. Aviation Week & Space Technology, November 22, 2004, pp. 24-26.
5. He, X. H. and Chen Y.S. “Hypersonic Engine”. Winged Missiles Journal, 2008, No.12, pp. 33-36.
6. Cohen, B. and Natan, B. “Experimental Investigation of a Supersonic Combustion Solid Fuel Ramjet”. AIAA paper 97-3237, AIAA/ASME/SAE/ASEE Joint Propulsion Conference & Exhibit, 33rd, Seattle, WA, July 6-9, 1997.
7. Shimon, S. and Alon Gany. “Testing Metallized Solid Fuel Scramjet Combustion”. XVIII International Symposium on Air Breathing Engines, September 2-7, 2007, Beijing, China.
8. Ben-Yakar, A. and Alon Gany. “Experimental Study of a Solid Fuel Scramjet”. Journal of Propulsion and Power, Vol. 14, N0.4, 1998, pp. 447-455
9. Merrill W.Becksteada, Karthik Puduppakkama, Piyush Thakreb, igorYangb,_ aBrigham Modeling of combustion and ignition of solid-propellant ingredients Young University, Provo, UT 84602, USA The Pennsylvania State University, 104 Research Building East, University Park, PA 16802, USA Received 4 May 2006; accepted 2 February 2007Available online 11 April 2007
10. *Handbook of Arty Weapon, Pt I*, Royal Military College of Sc, UK, 2.4 – 2.5, (1982).
11. *Brassey's Encyclopedia of Land Forces & Warfare*, Brassey's pub, UK, 110-111, (2002).
12. *US Army Material Command Pamphlet 706-106*, 3.23 – 3.24, (1969).

13. MacLaren A J et-al, Solid rocket motor space launch vehicles, *Acta Astronautica*, **30**, 165-172, (**1993**).
14. Technologies for Future Precision Strike Missile Systems - Missile Aeromechanics Technology, Fleeman EL, Paper presented at the RTO SCI Lecture Series on "Technologies for Future Precision Strike Missile Systems", held in Atlanta, USA, 23-24 March 2000; Turin, Italy, 3-4 April 2000; Ankara, Turkey, 6-7 April 2000, and published in RTO-EN-13.
15. J.-F. Guery et-al, Solid propulsion for space applications: An updated roadmap, *Acta Astronautica*, 66, 201- 219, (**2010**).
16. Gupta S C et-al, Evolution of Indian launch vehicle technologies, *Current Science*, 93(**12**), 1697-1714, (**2007**).
17. Lipanov A M, Historical Survey of Solid Propellant Rocket Development in Russia, *Jn of Prop and Power*, 19 (**6**), 1063-1088, Nov-Dec (**2003**).
18. Rossi C et-al, Design, Fabrication & Modeling of Solid Propellant : Microrocket-application to Microprop, *Jn of Sensors & Actuators,* 99, 125 – 133 (**2002**).
19. Nair UR et-al, Advances in High EnergyMaterials, *Def Sc Jr*, 60(**2**), 137-151, Mar (**2010**).
20. Tarver CM et-al, Initiation of an CL-20-Estane formulations, *Proceed: AIP conf*, 370, 891-941, (**996**).
21. Tian Y et-al, Study on formulation of CL-20, Proceedings of 4th Int Autumn Seminar on *Propellants, Explo & Pyrotechnics*, Shaoxing, China, 43-47, (**2001**).
22. Florczak B, A comparison of Al composite propellants containing HMX & FOX-7. *Central Euro J. Engineering Mater*, 5(**3-4**), 110-111, (**2008**).
23. Florczak B, Investigation of an Al binder/AP composite propellant containing FOX-7, *Central Euro J. Engineering Mater*, 5(**3-4**), 65-75, (**2008**).
24. Mueller D, New gun propellant with CL-20,Propellants Explo & Pyrotechnics, 24, 176-181, (**1999**).
25. Chen JK, Thermal decompo of energetic matls, kinetics & near surface products of azide polymersAMMO, BAMO and GAP in simulated combustion, *Combustion and Flame*, 87, 157- 168, (**1991**).
26. Hsieh WH, Combustion behavior of boron based BAMO/NMMO fuel rich solid propellants, *Journal of Propulsion*, 7(**4**), 497-504, (**1994**).
27. Châtillon C, Two-phase unsteady flow in solid rocket motors, *Aerospace Science and Technology*, 6, 413–422, (**2002**).
28. Mahanta Abhay K et-al, Recent Advances in Development of Eco-friendly Solid Composite Propellants for Rocket Propulsion, *Research Jr of Chem & Environment,* 14 (**3**), Sep (**2010**).
29. Shekhar H, Design of Funnel Port Tubular Propellant Grain for Neutral Burning Profile in Rockets, *Defense Sc Journal*, 59 (**5**), 494 – 498, Sep (**2009**).
30. *TBBG Pt II*, Her Majesty Stationary Office, (**1**), 238-239, (**1987**).
31. Egon G et-al, *Analysis and test methods for service life prediction of energetic materials*. Proceedings of 31st International Conferecne of ICT, Karlruhe, Germany, 149-1 to 149-11 June 27-30, (**2000**).
32. Shekhar H, Assessment of Poisson's Ratio for Hydroxy-terminated Polybutadine-based Solid Rkt Prop, *Defence Science Journal*, 60(**5**), 497-501, Sep (**2010**).
33. Miloš P, Geometry optimization of star shapedpropellant grain with special attention to minimization of stress and strain, *FME Transactions*, 35, 35-40,(**2007**).
34. *Textbook of Ballistics and Gunnery Part I*, Her Majesty Stationary Office, (**1**), 4 - 5, (**1987**).
35. Yahya SM, *Fundamentals of Compressible Flow with Aircraft and Rocket Propulsion*, New Age International Publishers, 530, (**2005**).
36. Shekhar H, Estimation of pressure index & temp sensitivity coeff of solid rkt prop by static evaluation, *Defence Science Journal*, 59(**6**), 666-669, Nov (**2009**).
37. http://www.wordiq.com/definition/Solid_rocket.
38. Gunnapure GS, Dissertation on 'Catastrophic Failure of Rocket Motor of Rocket Ammunition', ME Mechanical (Weapon), University of Pune, June 2004.
39. *Handbook of Arty Weapon, Pt II*, Royal Military College of Sc, UK, 22.4 – 22.5, (**1982**).
40. P. Bose and K.M. Pandey, Recent Advances in Solid Fuels for Rockets of Multi Barrel Rocket Launchers, IRACST – Engineering Science and Technology: An International Journal (ESTIJ), ISSN: 2250-3498, Vol.2, No.1, 2012, PP. 83-89.
41. K.M.Pandey and P. Bose, "Star Shape Solid Propellant Grain for Multi Barrel Rocket Launcher Application, "Accepted in International Review of Aerospace Engineering - Praise worthy prize publications, Italy.

This page is intentionally left blank